13A.10 Estimating Moist Static Energy and Surface Enthalpy Flux Variance in a Mature Hurricane: Modeling and an Observational Case Study

Jacob D. Carstens*, Michael V. Kopelman, and Allison A. Wing
Florida State University, Tallahassee, Florida

1. INTRODUCTION

Differential radiative and surface enthalpy fluxes are important in tropical cyclone (TC) genesis and intensification. One likely mechanism for the hypothesized overnight convective maximum in TCs is differential longwave radiative cooling between the TC, with deep convective clouds and an expansive cirrus outflow canopy, and its relatively clear outer environment. This, along with processes such as wind-induced surface heat exchange (WISHE, Rotunno and Emanuel 1987), amplifies the spatial variability of moist static energy (MSE).

Similar mechanisms contribute to the spontaneous “self-aggregation” of tropical convection. These feedback processes can be quantified using the budget equation for the spatial variance of MSE developed by Wing and Emanuel (2014). Notably, they have been shown to aid in both TC genesis and intensification in idealized modeling studies (Wing et al. 2016; Muller and Romps 2018; Carstens and Wing 2020). This provides an intriguing avenue to use the MSE variance budget and its relevant feedbacks to analyze and forecast real TCs.

This study evaluates our ability to characterize the variability of radiative and surface enthalpy fluxes, as well as MSE, using a sparse set of observations. It is a contribution to the TC Diurnal Cycle portion of the 2020 Hurricane Field Program. It represents one of the first attempts to apply the MSE budget perspective to an observed hurricane, examining the intricate interplay between convection and TCs.

2. MODEL AND OBSERVATIONS

We first use cloud-resolving model (CRM) simulations from the System for Atmospheric Modeling, version 6.8.2 (SAM, Khairoutdinov and Randall 2003). Cases include an abnormally large and small TC, and an asymmetric, slowly-intensifying TC. Several grid points are chosen to represent dropsonde launch points, which sample the full tropospheric column without any advection (Figure 1). From this, the model calculates fluxes of longwave and shortwave radiation, the column-integrated MSE, and surface latent and sensible heat fluxes to complete the diabatic components of the MSE variance budget. By varying the number of grid points used in the calculation and their spatial distribution across simulated “flight paths”, we evaluate how well the MSE variance and its feedbacks are captured by the small set of grid points relative to the full domain.

*Corresponding author information: Jacob D. Carstens, Department of Earth, Ocean, and Atmospheric Science, Florida State University, 1011 Academic Way, Tallahassee, FL 32306; Email: jcarstens@fsu.edu

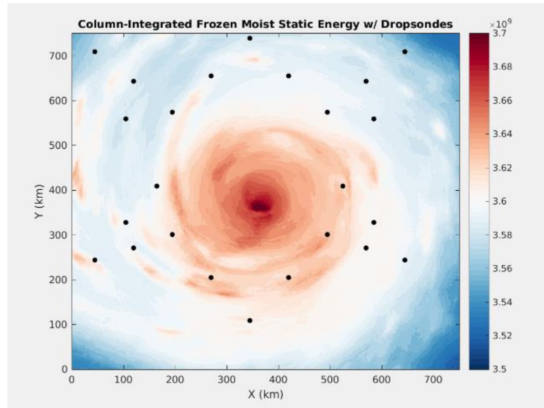

Figure 1: *Example of a star-shaped simulated flight pattern in SAM. Circles represent dropsonde launch points, overlaid on a map of column-integrated MSE.*

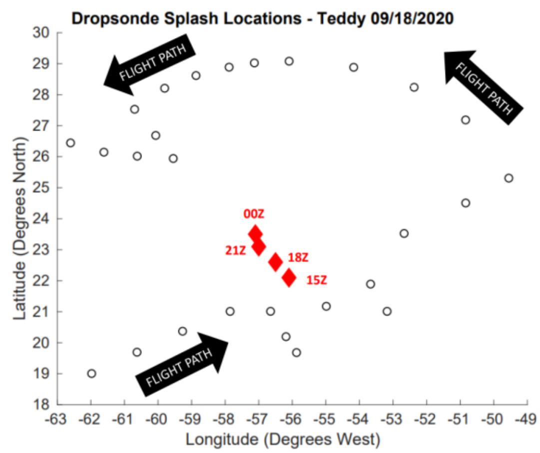

Figure 2: *Map of dropsonde splash points during upper-level reconnaissance mission for Teddy, 18 September 2020. Red diamonds represent center locations based on National Hurricane Center advisories and ATCF best track files.*

Dropsondes from the NOAA upper-air reconnaissance mission of TC Teddy on 18 September 2020 are used for initial observational analysis. With fine temporal and vertical resolution, this data allows us to estimate the MSE through a deep column of the troposphere. Three flight legs each served a different purpose: Transect legs to measure radial gradients of properties like MSE, star legs to sample differences between the near and far TC environments, and an arc near Teddy’s outflow jet (Figure 2). Going forward, this dataset is beginning to expand with a series of missions over TC Sally, and several others are planned.

3. MODELING RESULTS

Figure 3 shows the MSE variance and its diabatic feedbacks for the control simulation, for a series of simulated flight patterns varying in shape and "dropsonde" distribution. Clear differences emerge, but in general, the signs of feedback terms are correct and MSE variance is captured reasonably well. The longwave and surface flux feedbacks are the strongest contributors to MSE variance, amplifying the MSE where it is already high (i.e. near the TC) and decreasing it where it is lower (i.e. in the outer environment). Decomposition of these feedbacks reveals that they are predominantly differential cloud longwave cooling and WISHE.

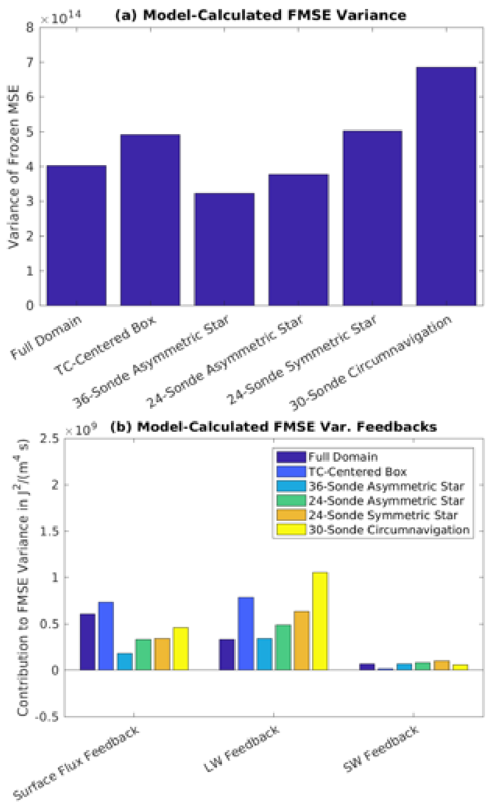

Figure 3: *(a) MSE variance computed across a series of simulated flight patterns in a SAM simulation. (b) Diabatic feedbacks to the MSE variance in the same TC. These are compared to values computed from the full domain, as well as a smaller TC-centered box.*

Linear transect patterns through the TC center resolve the MSE and radiative fluxes quite well outside the inner core. However, they are less effective in depicting surface fluxes and miss extrema in the eye (Figure 4). Therefore, it is likely that a more accurate sampling of the MSE variability and its tendency requires data in the eye and eyewall of the TC. Nonetheless, the model results present an encouraging outlook to apply this methodology to observed TCs.

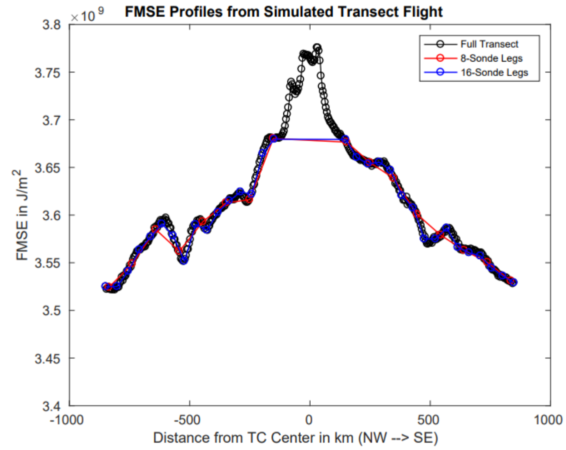

Figure 4: *MSE transect radial profiles in a SAM simulation, comparing different dropsonde densities to the computation using all possible grid points.*

4. TC TEDDY AND SALLY

Figure 5 depicts the radial profile MSE, computed from a moving TC center, for Teddy. A reduction in mid-troposphere MSE is evident with increasing radius, likely due to a Saharan Air Layer (SAL) at Teddy's periphery. The column-integrated MSE decreases linearly with increasing radius as well, computed from 217 to 990 hPa. Additional dropsondes from three flights near Sally, conducted prior to its intensification into a Category 2 hurricane, are also used to calculate column-integrated MSE. This is particularly advantageous because as a weaker TC, radii within 150 km of the center were sampled much more thoroughly. Figure 6 reveals that the approximate linear decreasing trend of MSE continues when adding this inner-core data.

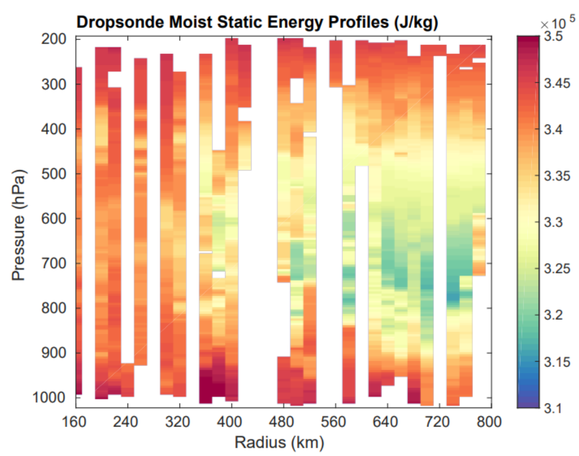

Figure 5: *Radius-pressure profile of MSE computed from all dropsondes deployed on 18 September 2020 upper-air mission over Teddy. Radius is composited into 20 km bins, and pressure into 15 hPa bins.*

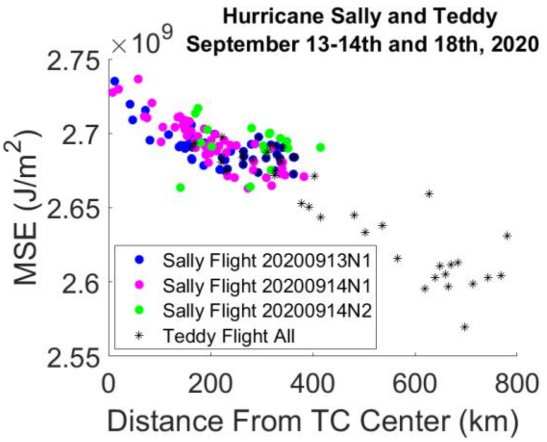

Figure 6: *Radial profile of column-integrated MSE for upper-air flights over TCs Teddy and Sally (2020).*

Work is underway to compute the spatial variance of MSE across these reconnaissance missions and an expanding dataset of observed Atlantic TCs. In addition, the potential exists to incorporate satellite data to estimate radiative fluxes and feedbacks, as well as SST and dropsonde splash measurements to compute surface enthalpy flux feedbacks. Finally, HWRF model forecasts will be incorporated as an important intermediate step in the analysis hierarchy, evaluating the potential usefulness of this methodology in real-time TC forecasting.

References

Carstens, J. D., and A. A. Wing, 2020: Tropical cyclogenesis from self-aggregated convection in numerical simulations of rotating radiative-convective equilibrium. *J. Adv. Model. Earth Syst*., **12**.

Khairoutdinov, M. F., and D. A. Randall, 2003: Cloud resolving modeling of the ARM summer 1997 IOP: Model formulation, results, uncertainties, and sensitivities. *J. Atmos. Sci*., **60**, 607–625.

Muller, C. J., and D. M. Romps, 2018: Acceleration of tropical cyclogenesis by self-aggregation feedbacks. *Proc. Nat. Acad. Sci*., **115**, 2930–2935.

Rotunno, R., and K. A. Emanuel, 1987: An air-sea interaction theory for tropical cyclones. Part II: Evolutionary study using a nonhydrostatic axisymmetric numerical model. *J. Atmos. Sci*., **44**, 542–561.

Wing, A. A., and K. A. Emanuel, 2014: Physical mechanisms controlling self-aggregation of convection in idealized numerical modeling simulations. *J. Adv. Model. Earth. Syst*., **6**, 59–74.

Wing, A. A., S. J. Camargo, and A. H. Sobel, 2016: Role of radiative-convective feedbacks in spontaneous tropical cyclogenesis in idealized numerical simulations. *J. Atmos. Sci*., **73**, 2633–2642.